DFT Calculations of EPR Parameters in an Ionic Lattice of $[M(CN)_4]^{3-}$ (M = Ni, Pd, Fe, Ru, Os) Complexes

Marcos C. Esteves,*,† Ney V. Vugman,‡ Alexandre A. Leitão,§ and Carlos E. Bielschowsky‡

Instituto de Química, Universidade Federal do Rio de Janeiro, Cidade Universitária, CT Bloco A, Rio de Janeiro, 21949-900 RJ, Brazil, Instituto de Física, Universidade Federal do Rio de Janeiro, Caixa Postal 68528, Rio de Janeiro, 21945-970 RJ, Brazil, and Departamento de Química, Universidade Federal de Juiz de Fora, Juiz de Fora, 36036-330 MG, Brazil

Received: January 9, 2007; In Final Form: May 8, 2007

The electronic *g*-tensor and hyperfine coupling constants were calculated for cyanide coordination complexes $[M(CN)_4]^{3-}$ (M = Ni, Pd, Fe, Ru, Os) in KCl or NaCl host lattices through an embedded calculation approach using the Density Functional Theory and compared with previous experiments. For all tested complexes, the B3LYP functional is in good agreement with the experiments for the hyperfine coupling constants. For the electronic *g*-tensor calculations, performed using the coupled perturbed SCF theory, some discrepancies were found, and the best agreements with the experimental values were achieved by the B3LYP functional.

I. Introduction

Systems with unpaired electrons play a very important role in chemistry and physics. They are present in cell metabolism,[1] combustion processes, catalytic intermediates,[2] and in magnetic phenomena taking place in active sites of important enzymes.[3] Electronic and conformational information of these systems may be obtained by Electron Paramagnetic Resonance (EPR) spectroscopy.[4] From the theoretical viewpoint, the use of quantum chemistry methods for the calculation of the EPR parameters allows a better understanding of their electronic structure, while their comparison with the experimental data may expand our capacity to predict these parameters using computational methods.

The isotropic hyperfine coupling (A_{iso}), an EPR parameter mostly dependent on the ground-state wave functions and derived from the *A* tensor, has already been calculated in good agreement with experiments using post-Hartree−Fock methodologies[5−8] and the Density Functional Theory (DFT).[9−16] The electronic *g*-tensor, which depends on the mixture of several states through angular and spin−orbit couplings, still remains a great challenge for computational methods, particularly in larger systems. Several efforts have been made to improve the calculations of the *g*-tensor using a series of quantum chemistry methodologies.[17−19] Nowadays, *g*-tensor calculations using the DFT methodology allow the study of complexes containing transition metals or molecules with a larger number of atoms.[20−24] Other approaches to *g* values, such as the multireference configuration interaction (MR-CI), present much higher computational costs and are only used for small molecules.[17]

The calculation of the *g*-tensor components using the coupled perturbed SCF theory within the density functional theory (CP-DFT) was proposed by Neese[19] and implemented in the Gaussian package.[25] This implementation is important because it allows the calculation of the *g*-tensor without demanding methodologies of higher computational cost.

The systems studied in this work are paramagnetic impurities in ionic host lattices. This kind of system can be obtained when diamagnetic complexes are diluted in alkali halide host lattices and submitted to γ-ray, X-ray, or 2 MeV electron irradiation.[26] The matrix influence on the complex is, of course, an important factor that needs to be included in the theoretical model used to simulate EPR tensors in solids. The interaction between the ionic lattice and the impurities may be simulated by an embedded cluster methodology.[5,6,27−34]

Some of the most widely used quantum chemistry methodologies[35−38] have already been used to test the embedded cluster model. In a recent work of our group, the Møller−Plesset perturbation theory, based on the unrestricted spin Hartree−Fock determinant (UMP2), was applied to represent clusters with paramagnetic 3d metal complexes interacting with NaCl or the KCl host environment.[5] The same methodology was also successfully used to calculate the A_{iso} values and the quadrupolar tensors for NaCl:$[Ni(CN)_4]^{3-}$ and KCl:$[Ni(CN)_4]^{3-}$. This previous theoretical experience suggests that $[Ni(CN)_4]^{3-}$ complexes in KCl and the NaCl host lattice may be very good probes for testing *g*-tensor calculations. Furthermore, the inclusion of other complexes in the discussion expands the range of the work, making the conclusions less dependent on the characteristics of a specific complex.

In this work, calculations of the hyperfine coupling constants and *g*-tensor are performed through an embedded cluster calculation for the following systems: NaCl:$[Ni(CN)_4]^{3-}$, KCl:$[Ni(CN)_4]^{3-}$, NaCl:$[Pd(CN)_4]^{3-}$, KCl:$[Pd(CN)_4]^{3-}$, NaCl:$[Fe(CN)_4]^{3-}$, KCl:$[Fe(CN)_4]^{3-}$, KCl:$[Ru(CN)_4]^{3-}$, and KCl:$[Os(CN)_4]^{3-}$.

II. Methodology

The hyperfine coupling constants (EPR parameter derived from the hyperfine coupling tensor) and the *g*-tensor were calculated for the different coordination complexes in KCl and NaCl host lattices using the Gaussian 03 Package[25] with an embedded cluster model. In our model, the cyanide complexes $[M(CN)_4]^{3-}$ (M = Ni, Pd, Fe, Ru, Os) are represented by a cluster containing two chlorines in axial positions embedded by 18 total ion potentials (TIPs) and 1306 point charges located in the corresponding pure crystal lattice position. The total ion

* Corresponding author phone: +55 21 2562-7462; e-mail: cabanas@iq.ufrj.br. Corresponding author address: Departamento de Físico-Química. Centro de Tecnologia, Bloco A, sala 304, Cidade Universitária, 21949-900 Rio de Janeiro - RJ, Brasil.

† Instituto de Química − Universidade Federal do Rio de Janeiro.

‡ Instituto de Física − Universidade Federal do Rio de Janeiro.

§ Departamento de Química - UFJF.

10.1021/jp0701845 CCC: $37.00
Published on Web 07/06/2007

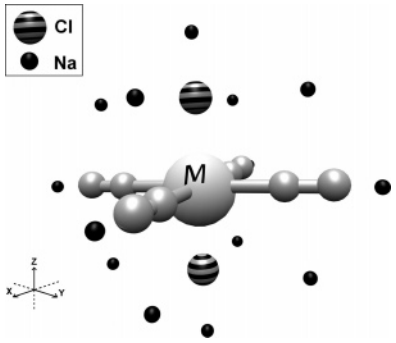

Figure 1. $[M(CN)_4Cl_2]^{5-}$ cluster embedded by 18 TIPs first neighbors.

potentials of K^+ or Na^+ surrounding the $[M(CN)_4Cl_2]^{5-}$ cluster (Figure 1) are represented by effective core potentials for the core of K and Na, and, due to the near crystal environment, they take into account the short-range potentials acting on the quantum-mechanical cluster. The point charge region is a cube of point charges, which contains 11 charges in the edge and which surrounds the cluster and the TIPs. Following the Evjen procedure,[39] ionic fractional charges were used at the borders of the cube to increase the convergence of the Madelung potential and to preserve system neutrality. The final symmetry of the systems was kept as D_{4h}. The embedded model described above is analogous to that reported in some previous references.[5,40]

The 6-311+G(d) basis set includes polarization and diffuse functions, needed to properly describe delocalized valence electrons of the complex bonding. The LANL2DZ basis set is adequate for transition atoms since it contains relativistic pseudopotentials. Nevertheless, the use of these pseudopotentials to represent the core electrons prevents us from calculating A_{iso} values for the metal, although experimental values are found in the literature.

The electronic structures were calculated within the DFT theory. Three different approximations were used for the exchange-correlation interactions: the local density approximation (LDA),[44] the generalized gradient approximation (PBE),[45,46] and the B3LYP hybrid functional.[47,48]

The isotropic hyperfine coupling constant (A_{iso}) was calculated multiplying the evaluated spin density at nucleus N by the nuclear g-factor (g_N), the free electron g-factor (g_e), the Bohr magneton (β_e), and the nuclear magneton (β_N):

$$A_{iso}^{N} = \frac{8\pi}{3h} g_e \beta_e g_N \beta_N \rho_{spin}(\vec{R}_N) \quad (1)$$

We used the Neese CP-DFT formulation to calculate g-tensor components of the complexes. According to Neese,[19] this involves four terms:

$$g_{rs} = g_e \delta_{rs} + \Delta g^{RMC} \delta_{rs} + \Delta g_{rs}^{GC} + \Delta g_{rs}^{OZ/SOC} \quad (2)$$

The first term is an isotropic contribution representing the free electron g value ($g_e = 2.002319$), and the second term is a relativistic mass correction term, introduced by Angstl[49] to correct the g values for planar aromatics complexes. This term is calculated with the ground-state spin density and kinetic energy integrals as

$$\Delta g^{RMC} = -\frac{\alpha^2}{S} \sum_{\mu,v} P_{\mu v}^{\alpha-\beta} \langle \varphi_\mu | \hat{T} | \varphi_\mu \rangle \quad (3)$$

where α is the fine structure constant, S is the total spin of ground state, $P_{\mu v}^{\alpha-\beta}$ is the spin density matrix, $\{\varphi\}$ is the basis set, and T is the kinetic energy operator.

The third term is a diamagnetic correction introduced by Stone[50] and is calculated with the ground-state spin density as

$$\Delta g_{rs}^{GC} = \frac{1}{2S} \sum_{\mu,v} P_{\mu v}^{\alpha-\beta} \left\langle \varphi_\mu \left| \sum_A \left[\frac{\alpha^2 Z_{eff}^{\ 4}}{2|r_i - R_A|^3} \right] (\vec{r}_A \vec{r}_O - \vec{r}_{A,s} \vec{r}_{O,s}) \right| \varphi_v \right\rangle \quad (4)$$

where $\vec{r}_A$ is the position vector of the electron relative to nucleus A, $\vec{r}_O$ is the position vector relative to the gauge origin, Z_{eff} is the effective nuclear charge, and the term in brackets is the effective spin−orbit coupling of the ith electron at A nucleus.

The fourth term is the dominant correction and comes as a crossed term between the Zeeman orbital (OZ) operator and the spin−orbit coupling (SOC). This term is calculated using the Neese's coupled perturbed theory with DFT methodology (CP-DFT).

III. Results and Discussion

Analysis of the g-tensors measured by EPR spectroscopy shows that the unpaired electron is in a $d_{x^2-y^2}$ (B_{1g}) orbital for d^9 complexes (M = Ni, Pd) and in a d_{z^2} (A_{1g}) orbital for d^7 complexes (M = Fe, Ru, Os).[26,51−56] All of our molecular orbital calculations led to the same conclusions: the HOMO of $d_{x^2-y^2}$ complexes presents an antibonding character in the region of the C−N bond, and the HOMO for d_{z^2} presents an antibonding character in the M−Cl region. The study of the symmetry and electronic density distribution of the unpaired electron is important due to their significant influence in the calculated geometries and in the A_{iso} and g-tensors values.

The following d^9 systems have been studied with the unpaired electron in the $d_{x^2-y^2}$ orbital: $NaCl:[Ni(CN)_4]^{3-}$, $NaCl:[Pd(CN)_4]^{3-}$, $KCl:[Ni(CN)_4]^{3-}$, and $KCl:[Pd(CN)_4]^{3-}$. The following d^7 systems with the unpaired electron in the d_{z^2} orbital have been studied: $NaCl:[Fe(CN)_4]^{3-}$, $KCl:[Fe(CN)_4]^{3-}$, $KCl:[Ru(CN)_4]^{3-}$, and $KCl:[Os(CN)_4]^{3-}$.

III.a - Geometry Optimization. No experimental values for the geometry of these complexes in ionic salt can be determined because they are dopants with very low concentration and do not appear in X-ray experiments. Therefore, geometry optimizations for all atoms in the clusters were performed (Figure 1) keeping the 1306 point charges and the TIPs fixed in the original positions. Table 1 shows the clusters optimized geometries with different exchange-correlation functionals, the results of which are discussed below.

In all systems, the M−Cl optimized bond distance was found to be close to the pure salt lattice internuclear values of 2.82 Å (NaCl lattice) and 3.15 Å (KCl lattice), with a mean variance of 3%. These values indicate that the chlorine ions near the metal are not chemically coordinated, reinforcing the assumption of a previous work.[5]

The M−CN optimized distances for 3d complexes are larger for the $d_{x^2-y^2}$ than for the d_{z^2} clusters, and this difference is attributed to the presence of an antibonding unpaired orbital in the cyanide plane of $d_{x^2-y^2}$ complexes. The B3LYP functional presents larger bond M−CN distances in comparison to other functionals. The same tendency was reported by other authors,[57−59] who attributed it to the absence of an adequate exchange interaction in LSD and PBE functionals in the description of the charge transference in the metal−ligands regions.

TABLE 1: Optimized Bond Distances within the Cluster (Å) Using Different DFT Functionals, a 6-311+g(d) Basis Set for C, N, and Cl Atoms, and a LanL2DZ Basis Set for Metals

system		LSD	PBE	B3LYP
NaCl:$[Ni(CN)_4]^{3-}$	Ni−CN	1.936	1.993	2.042
	Ni−Cl	2.814	2.902	2.913
	C−N	1.179	1.186	1.171
KCl:$[Ni(CN)_4]^{3-}$	Ni−CN	1.973	2.055	2.131
	Ni−Cl	3.082	3.202	3.218
	C−N	1.183	1.190	1.175
NaCl:$[Pd(CN)_4]^{3-}$	Pd−CN	2.077	2.116	2.145
	Pd−Cl	2.919	2.984	2.993
	C−N	1.172	1.180	1.165
KCl:$[Pd(CN)_4]^{3-}$	Pd−CN	2.136	2.199	2.249
	Pd−Cl	3.170	3.262	3.270
	C−N	1.178	1.187	1.172
NaCl:$[Fe(CN)_4]^{3-}$	Fe−CN	1.830	1.875	1.915
	Fe−Cl	2.722	2.844	2.875
	C−N	1.189	1.196	1.179
KCl:$[Fe(CN)_4]^{3-}$	Fe−CN	1.851	1.903	1.953
	Fe−Cl	2.949	3.139	3.180
	C−N	1.191	1.199	1.182
KCl:$[Ru(CN)_4]^{3-}$	Ru−CN	2.001	2.038	2.065
	Ru−Cl	3.006	3.166	3.208
	C−N	1.188	1.196	1.180
KCl:$[Os(CN)_4]^{3-}$	Os−CN	1.996	2.024	2.040
	Os−Cl	3.025	3.173	3.215
	C−N	1.190	1.199	1.184

The C−N bond distances have not varied significantly in all calculations, demonstrating that the strong triple covalent bonds are not significantly influenced by the metal or by the surrounding ionic crystals. Nevertheless, Table 1 shows, in general, smaller values for the B3LYP functional.

III.b - Calculations of Hyperfine Coupling Constants. Table 2 shows the calculated parallel component of the hyperfine coupling tensor (T_{zz}) and the A_{iso} values for the carbon, the nitrogen, and the two chlorines in the different clusters.

The $d_{x^2-y^2}$ (B_{1g}) unpaired electron systems with an antibonding orbital in the cyanide plane show larger values for the ^{13}C and ^{14}N A_{iso} and smaller ones for the ^{35}Cl nuclei. The d_{z^2} (A_{1g}) systems show larger values for the ^{35}Cl A_{iso}, due to the presence of the unpaired electron in the M−Cl direction, and smaller ones for A_{iso} for the equatorial ^{13}C and ^{14}N nuclei. Table 2 shows that the isotropic hyperfine couplings calculated by the DFT method with the B3LYP functional are closer to the experimental values in almost all cases. In two cases only, the PBE approximation showed the best theoretical values, and the LSD approximation was not suitable for any systems.

Figures 2 and 3 show the dependence of A_{iso}, calculated using the B3LYP functional, with some of the bond distances in the cyanide coordination complexes. In the $d_{x^2-y^2}$ systems, A_{iso} values are much more sensitive to the carbon and nitrogen coordinates within the molecular plane than to the axial chlorine coordinates. In the d_{z^2} systems, A_{iso} values are more sensitive to metal−chlorine bond distances than to metal-to-carbon and metal-to-nitrogen bond distances. The small variations observed in the chlorine A_{iso} reinforce the assumption that the chlorine ions near the metal are not chemically coordinated.

The quality of A_{iso} calculations also depends on $<S^2>$ values since this parameter monitors the contamination owing to other multiplicity states. The calculated $<S^2>$ values were around 0.76, indicating that, for all the systems, the spin contamination in the wave functions calculated for the three functionals is small enough. Thus, spin contamination is not responsible for the differences in the A_{iso} values shown in Table 2.

Another relevant factor for the A_{iso} computation is the choice of the basis set. Table 3 demonstrates that for small basis sets (6-31G) the calculated value for the nitrogen atom does not agree with experimental data—presenting a mean error of 30%—while for the others atoms A_{iso} achieves an acceptable accuracy. The results in nitrogen are improved using a basis set which permits more flexibility (6-311G), reducing the mean error to 17%. Nevertheless, the inclusion of diffuse functions and polarizable functions—necessary to properly describe bonding of the delocalized valence electrons—further reduces the mean error in nitrogen to 14%. Even if some references show that the Barone[60] (EPR-III) is the best basis set for A_{iso} calculations, we chose to use the 6-311+g(d) basis set because the EPR-III basis set is applicable only to hydrogen and some second row elements.

TABLE 2: Calculated and Experimental Values for T_{zz} and A_{iso} Using a B3LYP Functional, a 6-311+g(d) Basis Set for C, N, and Cl Atoms, and a LanL2DZ Basis Set for Metals (in MHz)[a]

system		LSD	PBE	B3LYP	exp
NaCl:$[Ni(CN)_4]^{3-}$	A_{iso} (C)	178.9	153.0	108.0	
	A_{iso} (N)	11.4	8.9	7.3	7.7[b]
	A_{iso} (Cl)	−3.0	−2.8	−3.7	>(−5)[b]
KCl:$[Ni(CN)_4]^{3-}$	A_{iso} (C)	174.6	140.1	89.3	105[c]
	A_{iso} (N)	10.5	7.6	5.5	6.8[b]
	A_{iso} (Cl)	−2.2	−2.0	−2.2	>(−4)[b]
NaCl:$[Fe(CN)_4]^{3-}$	A_{iso}(C)	−19.4	−24.7	−24.9	
	A_{iso} (N)	1.0	0.5	−0.0	
	A_{iso} (Cl)	52.4	34.7	29.8	28.2[d]
	T_{zz} (Cl)	19.7	13.6	9.9	7.5[d]
KCl:$[Fe(CN)_4]^{3-}$	A_{iso}(C)	−22.2	−27.0	−25.3	
	A_{iso}(N)	0.7	0.3	−0.2	
	A_{iso} (Cl)	33.4	18.9	15.8	17.0[e]
	T_{zz} (Cl)	13.7	8.2	5.9	6.8[e]
KCl:$[Ru(CN)_4]^{3-}$	A_{iso}(C)	−8.8	−11.3	14.0	
	A_{iso}(N)	1.1	0.8	0.7	
	A_{iso} (Cl)	59.2	38.2	33.9	29.0[f]
	T_{zz} (Cl)	25.2	18.4	14.0	12.9[f]
KCl:$[Os(CN)_4]^{3-}$	A_{iso}(C)	−9.3	−10.7	−11.9	
	A_{iso}(N)	0.4	0.2	0.1	
	A_{iso} (Cl)	71.0	48.0	44.0	37.8[g]
	T_{zz} (Cl)	29.4	22.5	18.2	19.2[g]
NaCl:$[Pd(CN)_4]^{3-}$	A_{iso} (C)	196.2	182.2	163.6	
	A_{iso} (N)	12.9	10.2	8.6	
	A_{iso} (Cl)	−1.4	−1.3	−1.7	
NaCl:$[Pd(CN)_4]^{3-}$	A_{iso} (C)	200.1	193.5	182.5	
	A_{iso} (N)	14.9	12.8	11.6	
	A_{iso} (Cl)	−2.0	−1.9	−2.4	

[a] T_{zz} is the z component of the dipolar hyperfine tensor. [b] Reference 5. [c] Reference 26. [d] Reference 51. [e] Reference 52. [f] Reference 53. [g] Reference 54.

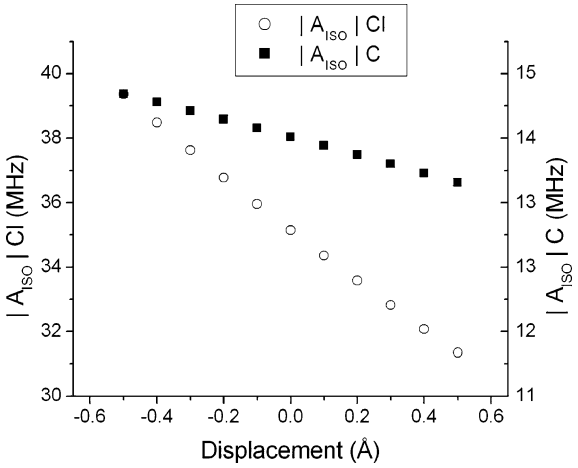

Figure 2. A_{iso} variance of ^{13}C and ^{35}Cl in the NaCl:$[Fe(CN)_4]^{3-}$ system. Calculated values for $|A_{iso}|$ in carbon refer to the variation in the Fe−CN bond distance and for chlorine to the variation in the Fe−Cl bond distance.

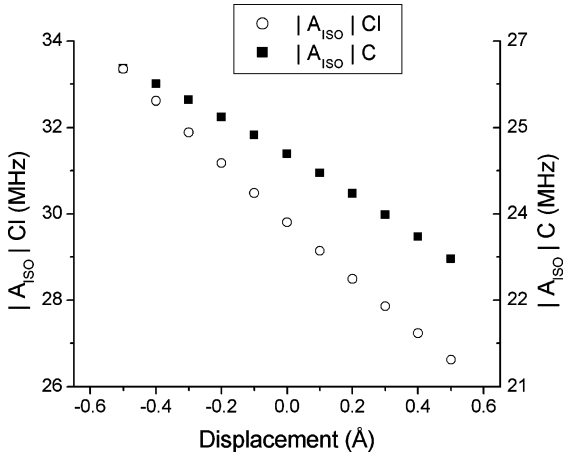

Figure 3. A_{iso} variance of ^{13}C and ^{35}Cl in the KCl:$[Ru(CN)_4]^{3-}$ system. Calculated values for $|A_{iso}|$ in carbon refer to the variation in the Ru−CN bond distance and for chlorine to the variation in the Ru−Cl bond distance.

TABLE 3: Values of A_{iso} Using a B3LYP Functional and Different Basis Sets

system	A_{iso}	6-31G	6-31+G(d)	6-311G	6-311+G(d)	exp
NaCl:$[Ni(CN)_4]^{3-}$	^{13}C	111.5	106.1	109.3	108.0	
	^{14}N	5.1	5.7	6.9	7.3	7.7[a]
	^{35}Cl	−3.0	−2.9	−2.9	−3.7	>(−5)[a]
KCl:$[Ni(CN)_4]^{3-}$	^{13}C	89.2	85.8	89.6	89.3	105[b]
	^{14}N	3.8	4.4	5.1	5.5	6.8[a]
	^{35}Cl	−2.2	−2.1	−2.0	−2.2	>(−4)[a]
KCl:$[Pd(CN)_4]^{3-}$	^{13}C	158.2	152.8	160.2	163.6	
	^{14}N	7.3	7.8	8.7	8.6	
	^{35}Cl	−1.7	−1.6	−1.7	−1.7	
NaCl:$[Pd(CN)_4]^{3-}$	^{13}C	182.5	175.2	180.3	182.5	
	^{14}N	9.4	10.1	11.5	11.7	
	^{35}Cl	−2.4	−2.2	−2.5	−2.5	

[a] Reference 5. [b] Reference 26.

We have shown in a previous work[6] that the calculated A_{iso} values in a particular atom are critically dependent on the collaborative effect of the spin polarization of all the electrons in the atom. In the present calculations, these atoms are described with an appropriate Gaussian basis set (6-311+G(d)) which adds the variational freedom necessary to describe spin polarizations and to achieve a good agreement between the calculated and the experimental values. The importance of this spin-polarization is observed in our results: in spite of the SOMO for B_{1g} complexes presenting a nodal plane in the Cl region, nonzero values for A_{iso} are observed in this region. This polarization is not caused by direct spin polarization of the unpaired electron but instead only by spin polarization.

The only previous A_{iso} theoretical calculations for these complexes[6] were restricted to the NaCl:$[Ni(CN)_4]^{-5}$and KCl:$[Ni(CN)_4]^{-5}$systems and were performed with the Unrestricted Hartree−Fock method followed by the Møller−Plesset perturbation theory (UHF-MP2) within the embedded cluster model. The present DFT results are in better agreement with the experiments than the former UHF-MP2 calculations. When we compare our results with other recent theoretical calculations for A_{iso} in ionic crystals with lighter defects,[37,38] we find very similar results.

In this work, the results in Table 2 are in good general agreement with the theoretical and experimental results for A_{iso} when the B3LYP functional and the 6-311+G(d) basis set is used. This shows that the DFT calculations with an adequate description of the host crystal are able to correctly predict the A_{iso} values for this kind of system.

TABLE 4: Calculated and Experimental Δ*g*-Tensor Using a B3LYP Functional, a 6-311+g(d) Basis Set for C, N, and Cl Atoms, and a LanL2DZ Basis Set for Metals

system		LSD	PBE	B3LYP	exp
NaCl:$[Ni(CN)_4]^{3-}$	$\Delta g_{\|\|}$	−0.013	0.023	0.091	0.109[a]
	$\Delta g_{\perp}$	0.016	0.022	0.041	0.036[a]
KCl:$[Ni(CN)_4]^{3-}$	$\Delta g_{\|\|}$	0.007	0.048	0.128	0.130[b]
	$\Delta g_{\perp}$	0.018	0.028	0.052	0.040[b]
NaCl:$[Pd(CN)_4]^{3-}$	$\Delta g_{\|\|}$	−0.113	−0.043	0.050	0.076[c]
	$\Delta g_{\perp}$	0.007	0.016	0.034	0.019[c]
KCl:$[Pd(CN)_4]^{3-}$	$\Delta g_{\|\|}$	−0.046	0.030	0.143	0.099[c]
	$\Delta g_{\perp}$	0.015	0.029	0.057	0.024[c]
NaCl:$[Fe(CN)_4]^{3-}$	$\Delta g_{\|\|}$	0.000	−0.001	−0.004	−0.006[d]
	$\Delta g_{\perp}$	0.061	0.056	0.081	0.157[d]
KCl:$[Fe(CN)_4]^{3-}$	$\Delta g_{\|\|}$	0.000	−0.001	−0.004	−0.005[e]
	$\Delta g_{\perp}$	0.090	0.074	0.103	0.201[e]
KCl:$[Ru(CN)_4]^{3-}$	$\Delta g_{\|\|}$	0.002	0.002	0.001	−0.024[f]
	$\Delta g_{\perp}$	0.156	0.178	0.249	0.273[f]
KCl:$[Os(CN)_4]^{3-}$	$\Delta g_{\|\|}$	0.010	0.010	0.008	−0.131[g]
	$\Delta g_{\perp}$	0.442	0.501	0.687	0.612[g]

[a] Reference 55. [b] Reference 26. [c] Reference 56. [d] Reference 51. [e] Reference 52. [f] Reference 53. [g] Reference 54.

III.c - Calculations of the Electronic *g*-Tensor. Table 4 shows the $\Delta g_{\perp}$ and $\Delta g_{||}$ values calculated with the coupled perturbed SCF theory ($\Delta g = g - g_e$, where $g_e = 2.0023$ is the g value for the free electron). Although it is rather difficult to give a general interpretation for the Δg-tensor, some trends might be observed comparing theoretical and experimental results. When comparing these results, it is important to observe that the usual experimental error in the measurement of the X band EPR g factor for well resolved lines is 0.0005.

In our present calculations, the M−Cl direction defines the parallel direction and, consequently, the $g_{||}$ direction. The perpendicular plane, related to the $\Delta g_{\perp}$ values, is the M−$(CN)_4$ plane.

The functional that is in better agreement with the experimental g values is the B3LYP functional. This may indicate that the exchange part, present in the B3LYP functional, is important for describing the electronic structure of the systems under study.

Comparing the results, in general, the g-tensors for Ni and Pd ($d_{x^2-y^2}$) are in a better match to the experiments than the g-tensors for the Fe, Ru, and Os (d_{z^2}) complexes. The discrepancies in our results are due to a limitation in our embedded model, which does not describe correctly the transference of spin density from A_{1g} complexes to the near lattice, as proposed in some previous experimental works.[61]

Another consideration is that, in general, the Δg values are in lesser agreement with experimental data for heavier metals. This might indicate that the use of core potentials, which does not allow the polarization of inner-shell and inner-valence orbitals, alters the spin-density polarization and induces a worse description of the occurring physical phenomena.

There are no other theoretical calculations for the g-tensor of the complexes treated in the present work. When we compare our results with other recent theoretical calculations for defects in ionic crystals and surfaces, we either find very similar results in some cases[62,63] or better ones in others.[37,38] We infer that the results obtained for the g-tensor are still not accurate but indicate the possibility of calculating this parameter using an embedded cluster model.

IV. Summary and Conclusion

The electronic g-tensor and hyperfine coupling constants were calculated for KCl:$[M(CN)_4]^{3-}$ and NaCl:$[M(CN)_4]^{3-}$ (M = Ni,

Pd, Fe, Ru, Os) using the DFT theory involving three exchange-correlation functionals: LSD, PBE, and B3LYP. The lattice was represented through an embedded model detaining two layers. The first layer, represented by total ion potentials, describes the interactions between the complex and the nearest neighborhood; the second layer, represented by point charges, accounts for the long range interactions.

For each system studied, the coordinates of the metal, chlorine, carbon, and nitrogen atoms were optimized freezing the coordinates of the rest of the crystal at their original positions and employing the above-mentioned functionals. Some patterns were observed in the results: the optimized metal−chlorine bond distance is close to the pure salt lattice internuclear distance, indicating that chlorine ions near the metal are not chemically coordinated; the optimized metal−carbon bond distances changed significantly with the symmetry of the unpaired electron orbital, and so their values can be related to the presence or not of this antibonding orbital in the molecular plane. Carbon−nitrogen bond distances did not vary significantly in all calculations, demonstrating that the lattice potential does not affect this strong triple bond.

When a B3LYP functional is used, the calculated values for the isotropic hyperfine coupling (property derived from the *A* tensor) are in good agreement with experimental values. In the tensor *g* calculations some discrepancies were found, and the functional in better agreement with experimental values was B3LYP. The discrepancies found for heavier metals compounds may be attributed to the impossibility of our embedded model to describe correctly charge transferences between the cluster and the embedded atoms. The utilization of nonpolarizable effective core potentials, which do not describe inner shell orbitals polarization, may be another factor in explaining the discrepancies in the calculated *g* values.

Acknowledgment. The authors are indebted to Conselho Nacional de Desenvolvimento Científico e Tecnológico, CNPq, for a research fellowship (N.V.V. and C.E.B.) and to CAPES for a Ph.D. fellowship (M.C.E.).

References and Notes

(1) Frausto da Silva, J. J. R.; Willians, R. J. P. *The biological chemistry of Elements. The inorganic chemistry of life*; Clarendon Press: Oxford, 1994.
(2) Frey, P. A. *Chem. Rev.* **1990**, *90* (7), 1343.
(3) Menon, S.; Ragsdale, S. W. *Biochemistry* **1997**, *36* (28), 8484.
(4) Abragam, A.; Bleaney, B. *Electron Paramagnetic Resonance of Transition Ions*; Clarendon: Oxford, 1970.
(5) Leitão, A. A.; Coelho Neto, J. A.; Pinhal, N. M.; Bielschowsky, C. E.; Vugman, N. V. J. *Phys. Chem. A* **2001**, *105*, 614.
(6) Leitão, A. A.; Vugman, N. V.; Bielschowsky, C. E. *Chem. Phys. Lett.* **2000**, *321*, 269.
(7) Li, W. Z.; Huang, M. B. *J. Mol. Struct. (THEOCHEM)* **2003**, *636*, 1−3, 71.
(8) Kobayashi, K.; Nagase, S.; Dinse, K. *Chem. Phys. Lett.* **2003**, *377*, 1−2, 93.
(9) Hermosilla, L.; Calle, P.; Garcia de la Vega, J. M.; Sieiro, C. *J. Phys. Chem A* **2005**, *109*, 1114.
(10) Schrier, J.; Whaley, K. B. *J Phys. Chem. A* **2006**, *110*, 5386.
(11) Grein, F. *Chem. Phys. Lett.* **2006**, *418*, 1−3,100.
(12) Takada, T.; Tachikawa, H. *Int. J. Quantum Chem.* **2005**, *105*, 1, 79.
(13) Ionescu, E.; Reid, S. A. *J. Mol. Struct. (THEOCHEM)* **2005**, *725*, 1-3, 45.
(14) Hou, X. J.; Nguyen, M. T. *Chem. Phys.* **2005**, *310*, 1-*3*, 1.
(15) Rinkevicius, Z; Telyatnyk, L.; Vahtras, O.; Agren, H. J. *Chem. Phys.* **2004**, *121*, 7614.
(16) Honzíček, J.; Vinklárek, J.; Nachtigall, P. *Chem. Phys.* **2004**, *305*, 1-3, 291.
(17) Bruna, P. J.; Grein, F. *Int. J. Quantum Chem.* **2000**, *77*, 324.
(18) Neese, F. *Int. J. Quantum Chem.* **2001**, *83*, 3-4, 104.
(19) Neese, F. *J. Chem. Phys.* **2001**, *115*, 11080.
(20) Pauwels, E.; Van Speybroeck, V.; Waroquier, M. *Phys. Chem. A* **2006**, *110*, 6504.
(21) Di Valentin, C.; Scagnelli, A.; Pacchioni, G.; Risse, T.; Freund, H. J. *Surf. Sci.* **2006**, *600*, 12, 2434.
(22) Mattar, S. M. *Chem. Phys. Lett.* **2005**, *405*, 4-6, 382.
(23) Mattar, S. M.; Sanford, J.; Goodfellow, A. D. *Chem. Phys. Lett.* **2005**, *418*, 1-3, 30.
(24) Grein, F. *Chem. Phys.* **2004**, *296*, 1, 71.
(25) Frisch, M. J.; Trucks, G. W.; Schlegel, H. B.; Scuseria, G. E.; Robb, M. A.; Cheeseman, J. R.; Montgomery, J. A., Jr.; Vreven, T.; Kudin, K. N.; Burant, J. C.; Millam, J. M.; Iyengar, S. S.; Tomasi, J.; Barone, V.; Mennucci, B.; Cossi, M.; Scalmani, G.; Rega, N.; Petersson, G. A.; Nakatsuji, H.; Hada, M.; Ehara, M.; Toyota, K.; Fukuda, R.; Hasegawa, J.; Ishida, M.; Nakajima, T.; Honda, Y.; Kitao, O.; Nakai, H.; Klene, M.; Li, X.; Knox, J. E.; Hratchian, H. P.; Cross, J. B.; Bakken, V.; Adamo, C.; Jaramillo, J.; Gomperts, R.; Stratmann, R. E.; Yazyev, O.; Austin, A. J.; Cammi, R.; Pomelli, C.; Ochterski, J. W.; Ayala, P. Y.; Morokuma, K.; Voth, G. A.; Salvador, P.; Dannenberg, J. J.; Zakrzewski, V. G.; Dapprich, S.; Daniels, A. D.; Strain, M. C.; Farkas, O.; Malick, D. K.; Rabuck, A. D.; Raghavachari, K.; Foresman, J. B.; Ortiz, J. V.; Cui, Q.; Baboul, A. G.; Clifford, S.; Cioslowski, J.; Stefanov, B. B.; Liu, G.; Liashenko, A.; Piskorz, P.; Komaromi, I.; Martin, R. L.; Fox, D. J.; Keith, T.; Al-Laham, M. A.; Peng, C. Y.; Nanayakkara, A.; Challacombe, M.; Gill, P. M. W.; Johnson, B.; Chen, W.; Wong, M. W.; Gonzalez, C.; Pople, J. A. *Gaussian 03, Revision B.05*; Gaussian, Inc.: Wallingford, CT, 2004.
(26) Zanette, S. I.; Caride, A. O.; Danon, J. *J. Chem. Phys.* **1976**, *64*, 3381.
(27) Sousa, C.; Casanovas, J.; Rubio, J.; Illas, F. *J. Comput. Chem.* **1993**, *14*, 680.
(28) Aachi, J.-I.; Kosugui, N. *Bull. Chem. Soc. Jpn.* **1993**, *66*, 3314.
(29) Miyoshi, E.; Miyake, Y.; Katsuki, S.; Sakai, Y. *J. Mol. Struct. (THEOCHEM)* **1998**, *451*, 1-2, 81.
(30) Berrondo, M.; Rivas-Silva, J. F. *Int. J. Quantum Chem.* **1995**, *29*, 253.
(31) Winter, N. W.; Pitzer, R. M.; Temple, D. K. *J. Chem. Phys.* **1987**, *87*, 2945.
(32) Winter, N. W.; Pitzer, R. M.; Temple, D. K. *J. Chem. Phys.* **1987**, *86*, 3549.
(33) Ferrari, A. M.; Pacchioni, G. *J. Phys. Chem.* **1995**, *99*, 17010.
(34) Soave, R.; Ferrari, A. M.; Pacchioni, G. *J. Phys. Chem. B* **2001**, *105*, 9798.
(35) Fink, K. *Chem. Phys.* **2006**, *326*, 297.
(36) Satitkovitchai, K.; Pavlyukh, Y.; Hübner, W. *Phys. Rev. B* **2003**, *67*, 165413.
(37) Stevens, F.; Vrielinck, H.; Van Speybroeck, V.; Pauwels, E.; Callens, F.; Waroquier, M. *J. Phys. Chem. B* **2006**, *110*, 8204.
(38) Van Speybroeck, V.; Stevens, F.; Pauwels, E.; Vrielinck, H.; Callens, F.; Waroquier, M. *J. Phys. Chem. B* **2006**, *110*, 8218.
(39) Evjen, H. M. *Phys. Rev.* **1932**, *39*, 675.
(40) Leitão, A. A.; Vugman, N. V.; Bielschowsky, C. E. *J. Phys. Chem A* **2002**, *106*, 9569.
(41) Hay, P. J.; Wadt, W. R. *J. Chem. Phys.* **1985**, *82*, 270.
(42) Wadt, W. R.; Hay, P. J. *J. Chem. Phys.* **1985**, *82*, 284.
(43) Hay, P. J.; Wadt, W. R. *J. Chem. Phys.* **1985**, *82*, 299.
(44) Vosko, S. H.; Wilk, L.; Nusair, M. *Can. J. Phys* **1980**, *58*, 1200.
(45) Perdew, J. P.; Burke, K.; Ernzerhof, M. *Phys. Rev. Lett.* **1996**, *77*, 3865.
(46) Perdew, J. P.; Burke, K.; Ernzerhof, M. *Phys. Rev. Lett.* **1997**, *78*, 1396.
(47) Becke, A. D. *J. Chem. Phys.* **1993**, *98*, 5648.
(48) Lee, C.; Yang, W.; Parr, R. G. *Phys. Rev. B* **1988**, *37*, 785.
(49) Angstl, R. *Chem. Phys.* **1989**, *132*, 3, 435.
(50) Stone, A. J. *Proc. R. Soc. London, Ser. A* **1963**, *271*, 424.
(51) Jain, S. C.; Reddy, K. V.; Reddy, T. Rs. *J. Chem. Phys.* **1975**, *62*, 4366.
(52) Viswanath, A. K.; Rogers, M. T. *J. Chem Phys.* **1981**, *75*, 4183.
(53) Livi, C. P. M.S. Thesis, Centro Brasileiro de pesquisas física, Rio de Janeiro, 1977.
(54) Martins, S., Jr.; Vugman, N. V. *Chem. Phys. Lett.* **1987**, *141*, 6, 548.
(55) Vugman, N. V.; Amaral, M. R., Jr. *Phys. Rev. B* **1990**, *42*, 9837.
(56) Vugman, N. V.; Netto Grillo, M. L.; Jain, V. K. *Chem. Phys. Lett.* **1988**, *147*, 2-3, 241.
(57) Ziegler, T. *Can. J. Chem.* **1995**, *73*, 743.
(58) Jonas, V.; Thiel, W. J. *Chem. Phys.* **1995**, *102*, 8474.
(59) Koch, W.; Hertwig, R. H. *Encyclopedia of Computational Chemistry*; Schleyer, P. v. R., Editor-in-Chief; Wiley: Chichester, 1998.
(60) Barone, V. *Recent Advances in Density Functional Methods Part I*; Chong, D. P., Ed.; World Scientific Publ. Co.: Singapore, 1996.
(61) Pinhal, N. M.; Vugman, N. V. *J. Phys. C* **1985**, *18*, 6273.
(62) Atanasov, M.; Daul Claude, A.; Rohmer, M.; Venkatachalam, T. *Chem. Phy. Lett.* **2006**, *427*, 449.
(63) Di Valentin, C.; Scagnelli, A.; Pacchioni, G.; Risse, T.; Freund, H.-J. *Surf. Sci.* **2006**, *600*, 2434.